Published in final edited form as:
NMR Biomed. 2014 December ; 27(12): 1468–1478. doi:10.1002/nbm.3136.

Hyperpolarized Gas Diffusion MRI for the Study of Atelectasis and Acute Respiratory Distress Syndrome

Maurizio Cereda[a,*], **Yi Xin**[b], **Stephen Kadlecek**[b], **Hooman Hamedani**[b], **Jennia Rajaei**[b], **Justin Clapp**[b], and **Rahim R. Rizi**[b]

[a]Department of Anesthesiology and Critical Care, University of Pennsylvania, Philadelphia, PA, USA

[b]Department of Radiology, University of Pennsylvania, Philadelphia, PA, USA

Abstract

Considerable uncertainty remains about the best ventilator strategies for the mitigation of atelectasis and associated airspace stretch in patients with acute respiratory distress syndrome (ARDS). In addition to several immediate physiological effects, atelectasis increases the risk of ventilator-associated lung injury (VALI), which has been shown to significantly worsen ARDS outcomes. A number of lung imaging techniques have made substantial headway in clarifying the mechanisms of atelectasis. This paper reviews the contributions of CT, PET, and conventional MRI to understanding this phenomenon. In doing so, it also reveals several important shortcomings inherent to each of these approaches. Once these shortcomings have been made apparent, we describe how hyperpolarized gas magnetic resonance imaging (HP MRI)—a technique that is uniquely able to assess responses to mechanical ventilation and lung injury in peripheral airspaces—is poised to fill several of these knowledge gaps. The HP-MRI-derived apparent diffusion coefficient (ADC) quantifies the restriction of ^{3}He diffusion by peripheral airspaces, thereby obtaining pulmonary structural information at an extremely small scale. Lastly, this paper reports the results of a series of experiments that measured ADC in mechanically ventilated rats in order to investigate (i) the effect of atelectasis on ventilated airspaces; (ii) the relationship between positive end-expiratory pressure (PEEP), hysteresis, and the dimensions of peripheral airspaces; and (iii) the ability of PEEP and surfactant to reduce airspace dimensions after lung injury. An increase in ADC was found to be a marker of atelectasis-induced overdistension. With recruitment, higher airway pressures were shown to reduce stretch rather than worsen it. Moving forward, HP MRI has significant potential to shed further light on the atelectatic processes that occur during mechanical ventilation.

Keywords

ventilator-induced lung injury; alveolar recruitment; artificial respiration; magnetic resonance imaging; hyperpolarized gas; atelectasis

[*]Corresponding Author: Maurizio Cereda, MD, Department of Anesthesiology and Critical Care, Perelman School of Medicine at the University of Pennsylvania, Dulles 773, 3400 Spruce Street, Philadelphia, PA 19104-4283. Tel: (215) 300-1519, maurizio.cereda@uphs.upenn.edu.

Introduction

Atelectasis refers to the reversible collapse of peripheral airspaces, a common complication of mechanical ventilation (1). The effective management of atelectasis is an important factor in improving the outcomes of patients with acute respiratory distress syndrome (ARDS), a form of respiratory failure characterized by disseminated lung injury and hypoxemia (2) and defined by consensus criteria (3). Approximately 190,000 Americans contract ARDS each year (4), resulting in 60% two-year mortality (5) and a high rate of disability in survivors (6).

Imaging methodologies continue to play a crucial role in disclosing the factors leading to the generation of atelectasis, its physiologic consequences, and its effects on lung biology during mechanical ventilation. Several modalities have been employed to these ends, chiefly computed tomography (CT) (7-9) and positron emission tomography (PET)(10, 11), with a limited contribution from proton magnetic resonance imaging (MRI)(12). More recently, electrical impedance tomography (13) and lung ultrasound (14) have been introduced to aid in the bedside titration of ventilator settings.

An ideal imaging methodology for the productive examination of atelectasis and the broader spectrum of physiologic and biological effects of mechanical ventilation would fulfill a number of criteria. Such an approach would: a) be safe for ventilated and critically ill patients; b) have very short acquisition times; c) cause limited or no radiation exposure; d) allow longitudinal and follow up studies; e) quantify regional characteristics of the diseased lung; f) be responsive to rapid changes in patient conditions; g) allow imaging at different stages of the respiratory cycle and multiple acquisitions in the same session; h) integrate and spatially correlate morphological measurements (i.e. of the burden of atelectasis) with functional and metabolic abnormalities, possibly within the same image.

Unsurprisingly, no available imaging methodology meets this demanding array of conditions. As such, this paper will review the contributions made by various imaging approaches for the evaluation of atelectasis in mechanically ventilated patients as well as highlight the gaps of knowledge still remaining in this field of study. We will then describe the potential of hyperpolarized (HP) gas MRI to fill several of these gaps by providing novel information on the microstructural effects of atelectasis and mechanical ventilation. Lastly, we will present the results of a series of HP MRI experiments designed to clarify important atelectatic dynamics.

Clinical Relevance of Atelectasis

In ventilated patients, atelectasis is predictably observed shortly after induction of anesthesia and intubation (9, 15, 16). Studies in humans and animals have identified several mechanisms responsible for this complication, including monotonous artificial breathing with relatively low tidal volume (VT) (17), low lung capacity (18), and high inspired fractions of oxygen (19). In the supine ventilated patient, atelectasis is particularly prominent in the dorso-basilar lung regions (Figure 1)(20). Placing patients in the prone position—a potentially life-saving maneuver in severe ARDS patients (21)—reduces atelectasis and improves the distribution of ventilation (22). Management of atelectasis is

centered on the application of positive end-expiratory pressure (PEEP), intermittent deep breaths (or "sighs") (23, 24), and recruitment maneuvers (the intermittent application of high airway pressures) (25).

The direct physiological consequences of atelectasis—hypoxemia and low lung compliance—have obvious implications for immediate patient survival (1). Yet over the long term, atelectasis seems to cause additional detrimental effects. For one, atelectasis is implicated in the genesis of ventilator-associated lung injury (VALI) (26,27), a common ARDS complication. VALI is a form of pulmonary inflammation similar to ARDS that occurs when the ventilator applies excessive tissue stretch (28,29). ARDS patients have a reduced amount of ventilated parenchyma (the "baby lung") that is more easily overstretched (30) (Figure 2); consequently, low stretch ventilation with small tidal volumes is one of few approaches that increase ARDS survival (31). In addition, shear forces during tidal reopening of collapsed airspaces trigger an inflammatory response termed "atelectrauma" (32). Defining the relevance of these mechanisms in atelectasis is vital, as the sustained PEEP strategies that minimize atelectrauma have the potential to further stretch ventilated airspaces through increased inspiratory pressure, thereby worsening rather than improving VALI (33,34). This phenomenon could explain why studies designed to examine the clinical effects of high PEEP in ARDS have failed to show a clear survival benefit from this strategy when compared with standard management (35-37).

In clinical trials and in the majority of animal studies, mechanical responses to respiratory therapies such as VT selection and PEEP are evaluated using airway pressures (38), which have poor accuracy and lack topographic information. Measurements of lung volumes (39) and transpulmonary pressures are used to estimate global lung deformation or strain (40), but they do not provide spatial localization of the areas at risk of overstretch. To correct for the deficiencies of non-imaging approaches, various imaging techniques have been used to develop parameters for the more sensitive evaluation and management of atelectasis.

Structural Imaging in Mechanically Ventilated Lungs

Several prominent structural imaging techniques have been used to investigate the mechanics of ARDS and ventilator-related atelectasis. Concurrent to this progress, however, research using these techniques has revealed that they exhibit several important shortcomings.

While plain chest radiography is essential to ARDS diagnosis (3), it has low accuracy in detecting the early stages of disease (41) and does not capture the distribution of injury in three dimensions. CT of the lung has been favored by critical care physicians and investigators due to its ability to provide topographical and quantitative information (42,43). In fact, CT is capable of partitioning the lung into regions with different gas contents based on x-ray attenuation, thereby allowing measurement of the degree of atelectasis and edema (8,44,45). Early studies using CT highlighted the tremendous regional heterogeneity of lung injury and aeration in ARDS (46)(Figure 1). Ventilated parenchyma often has below-normal CT density (<-900 Hounsfield Units), suggesting airspace overdistension (33). Quantification of atelectasis in ARDS has prognostic value: in an observational study, the

amount of recruitable atelectatic tissue was an independent predictor of mortality that performed better than any clinical parameters (7). Sophisticated CT image analysis techniques can measure heterogeneities of aeration (47) and of regional tissue deformation (48) due to lung injury and respiratory maneuvers. However, CT provides limited functional information and causes substantial radiation exposure, limiting follow-up. More importantly, CT does not provide information on the sub-voxel distribution of gas (43) and on the mechanics of individual airspaces, which is critical to understanding the effects of mechanical ventilation.

Conventional MRI of ^{1}H nuclei has also been exploited for the quantification of atelectasis in ventilated humans (12). Although proton MRI is one of the best imaging modalities for longitudinal studies, its use in the lung is hindered by the low proton density of lung tissue, large susceptibility to artifacts, and inescapable cardiac and respiratory motions during image acquisition. Using ultra short echo time (UTE) imaging, it is possible to overcome the short T2* of lung parenchyma (49, 50). However, the signal-to-noise ratio of UTE remains challenging, and the technique also requires a fairly long acquisition time, increasing motion artifacts. In ARDS lungs, the local spin density of tissue can be dramatically increased by interstitial and alveolar edema or by massive atelectasis; as such, investigators have imaged lung water content or evaluated air-tissue interfaces (T2*) using gradient echo and spin echo techniques (51-54). More recently, MR elastometry has been used to map intrinsic elastic characteristics of lung tissue by measuring shear wave propagation during external mechanical stimulation (55). Using this technique, it has been shown that lung injury and edema do not increase parenchymal stiffness; low lung elastance can instead be explained by elevated surface forces in the airways (56). These important findings suggest that, in the future, ^{1}H MR techniques may allow detection of the early pathological changes caused by lung injury and evaluation of the effects of ventilation on the parenchyma.

Functional Imaging in Mechanically Ventilated Lungs

In recent years, functional imaging techniques have been introduced to the examination of atelectasis and ARDS. While a comprehensive review of these methodologies is beyond the scope of this article and can be found elsewhere (57, 58), it will suffice here to discuss the specific breakthroughs that have been made in investigating the regional abnormalities of lung function and metabolism that are characteristic of atelectasis and ARDS.

Considerable research effort has been invested in the development of techniques to image pulmonary ventilation (59). Ventilation can be mapped using methodologies that quantify regional lung expansion (60) or the kinetics of inhaled tracers such as Xe (61) or He (62). It is also possible to measure ventilation using oxygen-enhanced MRI (63,64). A recent study used synchrotron CT to obtain matching Xe-enhanced ventilation and density maps in surfactant-depleted rabbits (65). Xe-CT showed high ventilation in areas of the dependent lung with the characteristic density (between -500 and -100 HU) of poor aeration. PEEP redistributed inspired gas to normally aerated tissue. This study suggests that atelectatic and hyperventilated airspaces can be in close proximity to each other.

Positron emission tomography (PET) has been crucial to unlocking the mechanisms of hypoxemia in atelectasis and ARDS. Images of pulmonary water content and blood flow, obtained by measuring the distribution of injected $H_2{}^{15}O$, showed that dorsal areas of the lung are relatively more edematous but have well-preserved perfusion in patients with ARDS and pulmonary edema (66). By studying the kinetics of inhaled and injected $^{13}N_2$, it is possible to obtain matching maps of specific ventilation and regional blood flow, thus enabling the visualization of the spatial distribution of intrapulmonary shunt (i.e., lung with negligible ventilation but preserved perfusion). Shunt is mostly localized in the dorsal lung regions, which are poorly ventilated but relatively well perfused in supine subjects (67). Hypoxic vasoconstrictive responses, which usually divert blood flow away from hypoventilated airspaces, seem to be blunted in lung injury and in atelectasis, thus causing hypoxemia (68). Regional shunt is attenuated by maneuvers that improve the distribution of ventilation [recruitment (69), prone positioning (22)] and of perfusion [inhaled vasodilators (68)].

PET allows co-localization of functional abnormalities with areas of inflammation, thus enabling the study of the biological consequences of mechanical ventilation on a topographic basis. This task is accomplished by measuring the regional uptake and phosphorylation of injected [^{18}F]-fluoro-2-deoxy-D-glucose (18-FDG), which are related to neutrophil flow and activity. Through this methodology, early inflammatory changes due to high stretch ventilation were mapped in healthy lungs (70) and in animals with inflammation due to endotoxin infusion (71). Measurements of 18-FDG kinetics also showed inflammatory activation in areas of atelectasis due to surfactant depletion (10) and in healthy animals undergoing prolonged ventilation with low VT and no PEEP (11). In the latter study, increased 18-FDG uptake and phosphorylation were detected in dorsal lung regions that underwent progressive loss of aeration. These findings suggest the occurrence of early lung injury during prolonged ventilation with VT settings that are within clinical practice. Studies combining PET and CT are particularly relevant because they allow the precise correlation of functional and metabolic abnormalities with known morphological characteristics of lung injury. In ARDS patients, 18-FDG uptake and phosphorylation was higher in parenchyma that was well aerated by CT, thus confirming that these regions of the lungs are more susceptible to inflammation when exposed to excessive stretch (72).

While functional imaging will likely continue to expand our knowledge of atelectasis and ARDS, the shortcomings of these methodologies hinder their extensive clinical and investigational use in humans. These methods are extremely complex to employ, requiring highly specialized staff. Further, the scarcity and high expense of the requisite equipment—which is not available at all sites—and of the materials used (i.e. inhaled noble gases) pose an impediment. The radiation-related risk of these modalities (particularly PET) and their prolonged acquisition times also present safety risks. Lastly, functional imaging techniques face challenges related to a lack of unquestionable gold standards for validation and their often variable within-patient and inter-patient reproducibility.

Hyperpolarized Gas Diffusion MRI in Atelectasis and Lung Injury

HP MRI is not exempt from many of the abovementioned shortcomings; indeed, its operational complexity and the elevated cost of inhaled gas limit its widespread use. However, compared with PET, HP MRI has advantages including shorter acquisition times, higher spatial resolution, and lack of radiation exposure (73). More importantly, other imaging methodologies lack the unique ability of HP MRI to estimate the dimensions of airspaces distal to the terminal bronchiole (74), such as the alveoli and the alveolar ducts. This feature is extremely pertinent to the study of atelectasis and ARDS because it enables measuring regional responses to mechanical ventilation and lung injury in the most peripheral airspaces. Previously, there had been virtually no tools or techniques available to obtain direct measurements of airspace mechanics in a non-invasive manner (75). While adopting HP MRI for the management of intubated, critically ill patients is a distant objective, the approach offers a unique opportunity to test new hypotheses and challenge old dogmas on the physiology of mechanical ventilation.

HP noble gas MRI has in recent years unlocked new perspectives on lung imaging (76) and atelectasis. The diffusion of ^{3}He—a highly diffusive gas due to its low atomic mass—is restricted by the peripheral airspaces, and this restriction is quantified by its apparent diffusion coefficient (ADC) (77, 78). ADC measurements in the healthy lung are consistent with the sizes of the alveoli (∼200 μm in the case of humans, or ∼50 μm in the case of mice) and the alveolar ducts (74); it is likely that the former structures are more relevant to the observed ADC value, as they are highly represented within the acinus. In studies of the diseased lung, authors have reported a good correlation between ADC and pulmonary function or histology in chronic obstructive lung diseases (74, 79), and in aging (76, 80). As of yet, the use of HP MRI in ARDS is unexplored. However, it is notable that imaging can be performed during a single 3-second inspiratory breath hold, allowing the nearly instantaneous appreciation of the airspaces at the end of inspiration and in static conditions (after redistribution of inhaled gases has occurred) (81). This rapidity of execution allows the highly dynamic lung to be followed in real time and is necessary to study the effects of respiratory maneuvers.

In order to better understand the process of atelectatic formation and resolution and to inform strategies for the management of ARDS, we performed a series of HP MRI experiments using rodent models of atelectasis and lung injury (82-84). These experiments were designed to investigate: whether atelectasis worsens overdistension of ventilated airspaces; the spatial relationship between atelectatic regions and excessive stretch; how PEEP and recruitment maneuvers modify the dimensions and the hysteresis of the peripheral airspaces; and the effects of surfactant replacement on atelectasis and airspace stretch.

The imaging techniques used in our experiments on atelectasis and lung injury are described in detail in our published studies (82-84) and will be summarized in the current article. Briefly, ^{3}He was hyperpolarized through spin exchange collisions with optically pumped rubidium atoms to a level of 25∼30% (IGI.9600. He, GE Healthcare, Durham, NC). Due to the use of serial imaging in our experiments, prolonged polarization relaxation times ($T_{1,\,\mathrm{ext}} \approx 45$ min) were necessary and were obtained by placing the HP ^{3}He chamber inside the

magnet bore near the radiofrequency (RF) imaging coil. Imaging was performed on a 50-cm 4.7-T MRI scanner (Varian Inc., Palo Alto, CA) equipped with 12-cm 25 G/cm gradients and a quadrature 8-leg birdcage body RF coil with ID = 7 cm (Stark Contrast, Erlangen, Germany) tuned to the ^{3}He resonance frequency of 152.95 MHz. Animals were placed supine in the RF coil. Images were obtained after a series of five breaths with an 80%/20% mix of HP ^{3}He/oxygen to allow homogeneous distribution of tracer gas to hypoventilated airspaces (85). ^{3}He breathing was preceded by a series of inspirations with identical concentration of ^{4}He in oxygen to eliminate artifacts due to variability in alveolar gas concentrations at different PEEP levels (86). Animals were anesthetized, paralyzed, transorally intubated, and ventilated with a mechanical ventilator capable of mixing up to three different types of gases (e.g. ^{3}He, O_2, and air) at different ratios. The ventilator gas-handling unit was composed entirely of pneumatic and nonmagnetic delivery valves, placed as close as possible to the animal in order to minimize dead spaces and compression volume. PEEP was delivered and adjusted through a water valve connected to the exhaust line of the ventilator.

Atelectasis causes airspace stretch in healthy lungs

To document the effects of the progressive formation of atelectasis on ventilated airspaces, we performed serial HP MRI on healthy rats undergoing mechanical ventilation (82). The respiratory protocol was explicitly designed to cause atelectasis (87): animals were ventilated for prolonged periods with a moderate VT (10 ml/kg) and no PEEP. Recruitment maneuvers (performed by temporarily increasing PEEP) were performed intermittently to reopen atelectasis. By measuring inspiratory pressures, we were able to monitor lung mechanics and confirm the onset of progressive atelectasis during ventilation at zero PEEP (17) and its reversal by recruitment. Imaging was performed: before and after the recruitment maneuvers; at the beginning and at the end of each period of ventilation at zero PEEP; and at various intervals during mechanical ventilation (Figure 3). In this experiment, ADC was measured during two subsequent inspiratory holds performed after five breaths with HP ^{3}He; a double acquisition technique was used, consisting of the application of five different values (*b*) of bipolar diffusion-sensitizing gradients in opposite order during the two breath holds. Image acquisition was performed in the mid-lung coronal slice using a fast gradient echo pulse sequence with a field of view = 6 × 6 cm^2, slice thickness = 5 mm, flip angle $a \approx$ 4-5°, matrix size = 64×64 pixels, repetition time = 8.1 ms, and echo time = 3.3 ms. Diffusion weighting was performed in the phase-encode direction, using a diffusion time of 1 ms, a gradient duration of 200 μs, and b values of 0, 5.27, 3.09, 1.41, and 0 s/cm^2, with a ramp time of 180 μs. ADC maps were generated with a planar resolution of 0.94×0.94 mm^2 after correction for background noise and exclusion of pixels with inadequate signal-to-noise ratio. Each pixel was analyzed by fitting the evolution of signal to a standard equation (82).

The chief finding of this experiment (82) was a time-dependent (9.5% h^{-1}) increase of ADC signal during the periods of ventilation at zero PEEP. Recruitment maneuvers caused ADC to decrease by 21.2 ± 4.1 % and restored baseline ADC values. The images of Figure 3 document the decrease of ADC after recruitment, followed by an increased signal during the

subsequent 110-minute period of ventilation. The reversibility of the ADC elevation after recruitment strongly supports a causal relationship with atelectatic buildup.

At first, it appears surprising that the progression of atelectasis was associated with a higher ADC, as atelectasis is typically associated with smaller lung volumes (18). While monotonous ventilation with no PEEP could cause progressive reduction of airspace dimensions due to increasing surface forces, this was not picked up as decreased ADC. Because the larger ADC implies bigger individual airspaces, it can be argued that atelectasis promotes the progressive expansion of the ventilated airspaces. To explain this finding, it is useful to refer to a model of lung mechanics wherein two populations of airspaces coexist—atelectatic and ventilated (Figure 2). ADC only reflects the latter because collapsed parenchyma cannot be reached by inhaled HP gas (88, 89). During atelectatic buildup, the progressive loss of aerated tissue requires that all inspired gas goes to the residual functional airspaces, which dilate unless tidal volume is reduced (Figure 2). Furthermore, the forces of chest wall recoil and inter-alveolar traction (90) help maintain their opening. The simultaneous observation of improved mechanics after recruitment maneuvers implies an increased pool of ventilated units, which had smaller individual dimensions when measured by ADC. Indeed, ADC distributions were consistently skewed towards lower values after recruitment, a pattern that was associated with opening of smaller alveoli in microscopy studies (91). These data in healthy ventilated rats support a model whereby alveolar collapse is intimately related to overdistension and stretch. Although there is no evidence that this specific mechanism is the prominent cause of VALI, healthy rats ventilated similarly showed evidence of inflammation after a period of only 2.5 hours (87).

Recruitment Causes Pulmonary Hysteresis—It is well known that healthy lungs exhibit a hysteretic behavior: smaller distending pressures are required to maintain lung volume shortly after a deep breath (Figure 4)(92, 93). The specific mechanisms underlying this phenomenon are the subject of debate. In particular, it is not clear whether the peripheral airspaces exhibit an identical response to the whole lungs. If this were the case, larger airspace dimensions should be observed in the descending–vs. ascending—limb of an inflation-deflation cycle (94-96), as improved surfactant activity is expected to decrease surface tension and the elastance of individual airspaces (96). However, morphometry studies have suggested that peripheral airspaces may not mimic whole-lung responses: unchanged (97) or smaller-size (98) alveoli were detected with hysteresis. This behavior can only be explained if it is assumed that hysteretic changes in lung volume are due to a variation in the number, and not in the size, of individual open airspaces—i.e., hysteresis due to recruitment. Indeed, studies using intravital microscopy (99) and *in-vivo* HP MRI morphometry (100) have indicated that recruitment may be involved in lung expansion even in healthy subjects. Clarifying the mechanisms of hysteresis is clinically relevant: if airspace dimensions are reduced by hysteresis, setting PEEP after a deep inflation or RM could be a clinically useful approach to minimizing lung stretch and VALI (92, 101-103).

To investigate the relationship between hysteresis, PEEP, and peripheral airspace dimensions, we studied groups of healthy animals undergoing ramps of ascending followed by descending PEEP (83). Animals were anesthetized, intubated, monitored, and ventilated as described above. A recruitment maneuver was administered prior to the beginning of the

experiment to eliminate macroscopic atelectasis. PEEP was increased stepwise from zero up to 9 cmH_2O and was then returned to zero in identical steps. Imaging was performed during inspiratory breath holds at each PEEP level. Two groups of animals undergoing identical ventilatory protocols were studied. In one group, ADC was measured as previously described (82), except that images were acquired in a 20-mm-thick subcardiac axial slice. Furthermore, an interleaved diffusion-weighted gradient echo imaging pulse sequence was used, with all diffusion-sensitizing gradients applied during a single breath hold. In a separate group of animals, ventilator-gated inspiratory imaging was performed with a micro CT scanner to calculate end inspiratory lung volume (EILV). This was defined as the gas content of the lungs at end inspiration and was measured at each PEEP through quantitative analysis of three-dimensional whole-lung reconstructions (43, 104). This design allowed for the separation of the effects of hysteresis on individual ventilated airspaces (measured by HP MRI) from the effects on the whole lung (measured by CT).

The occurrence of whole-lung hysteresis was documented by larger lung volumes in descending vs. ascending ramps at matching PEEP levels (Figure 5 A): EILV was 8.4±2.8 versus 6.8±2.0 mL ($P<0.001$) in descending vs. descending PEEP. However, ADC values were smaller in the descending vs. the ascending ramp (Figure 5 B), amounting to 0.168±0.019 vs. 0.183±0.019 cm^2/s, respectively ($P<0.001$). Therefore, the hysteresis of ADC values was in opposite direction to that of the whole lung (Figure 6), suggesting smaller peripheral airspaces when EILV was larger. Furthermore, we observed a biphasic response of ADC to increasing PEEP: ADC increased 15.8% up to PEEP 6 cmH_2O and then decreased 3.6% when PEEP was further raised to 9 cmH_2O (Figure 6).

The smaller ADC values in the descending PEEP suggest that whole-lung hysteresis was likely due to reopening of increasing numbers of smaller airspaces rather than to the inflation of already open ones. We ascribed the findings of this study to recruitment of sub-voxel microatelectasis (105) when PEEP reached its highest value. This explanation was supported by a decrease of the fraction of lung tissue with poor aeration (between -500 and -100 Hounsfield Units by CT) at higher PEEP. Recruitment was then maintained during the descending PEEP ramp, thus generating the hysteresis. Newly recruited airspaces were smaller, likely because their individual distension was diluted by their increased number and because inter-alveolar traction forces were attenuated (90, 91).

An additional interesting result of this study was that changes of ADC due to PEEP and hysteresis were more prominent in the posterior regions of the lungs, which may indicate a concentration of tissue stressors in this area. Other authors detected inflammatory changes related to VALI in the posterior lung (11, 106, 107), making it possible that there is a link between ADC measurements of airspace dimensions and local propensity to injury.

PEEP decreases airspace stretch in injured lungs—To investigate the effects of the formation and resolution of atelectasis on ventilated airspaces in a model of lung injury, we measured ADC and CT densities during PEEP trials before and after surfactant depletion and following exogenous surfactant administration (84). Surfactant was depleted using pulmonary saline lavage, a model of lung injury with an extreme propensity to atelectasis (108). Rats were ventilated with VT of 10 ml/kg; PEEP was increased stepwise up to 9 or 15

cmH_2O (depending on study conditions) and imaging (CT or MRI, depending on group assignment) was performed at each level of PEEP tested. CT and HP MRI procedures were similar to the previously mentioned study on hysteresis (83), but ADC and CT images were acquired in anterior and posterior coronal slices to evaluate the regional (dorsal vs. ventral) effects of atelectasis.

After lavage, sparse aeration defects were visible on ^3He spin density maps (Figure 7A), suggesting a predominance of atelectatic airspaces in the imaged voxels, and ADC was 33% higher than in the normal lungs (Figure 7B). CT showed the expected increase in lung density (with over-representation of non-aerated and poorly aerated tissue) at zero PEEP (Figure 7C). PEEP 9 cmH_2O in healthy lungs (Figure 8) led to higher ADC, suggesting inflation of normal parenchyma. When PEEP was raised after saline lavage, aeration defects and CT density were decreased, confirming recruitment, but ADC was also reduced, suggesting reopening of newly recruited airspaces with smaller dimensions (Figure 8); despite higher airway pressures, PEEP did not cause volumetric expansion of previously open airspaces in surfactant-depleted lungs. Furthermore, the effects of PEEP on recruitment and ADC were facilitated—synergistically—by intratracheal administration of an exogenous surfactant formulation (BLES Biochemicals, London, Ontario, Canada). ADC decreased 23% in the presence of both surfactant and PEEP 9 cmH_2O. This phenomenon may be explained by enhanced recruitment (by surfactant) or by improved surfactant effect (109) and distribution (by recruitment) (110). In either case, surfactant had a sparing effect on both PEEP and inspiratory pressures.

In similar fashion to what we observed in our study on hysteresis (83), it is plausible that PEEP decreased distension of ventilated airspaces by increasing their number and releasing inter-alveolar forces. An interesting point raised by this study is the discrepant behavior of CT densities and ADC signal. In this study, ADC was abnormally high in conditions when CT density was also high. Furthermore, ADC signal was higher in the posterior lung, where CT density was higher – an expected finding since the animals were supine. Very low-density tissue (<-900 HU), thought to represent hyperinflated alveoli, was minimal and virtually absent at low PEEP, when ADC was the highest. These apparent discrepancies can be explained by the fact that the relationship between airspace volume and CT density is not univocal: CT provides limited insight into the mechanics of ventilated airspaces that neighbor collapsed units. Although it identifies regions with macroscopically hyperinflated parenchyma (38), CT may under-detect overstretched airspaces in voxels where they coexist with collapsed ones. A unique aspect of ADC is that this imaging parameter describes microstructures in such a way that the signal is weighted toward dilated airspaces. When collapsed airspaces are preponderant in a voxel, ^3He signal is low and the ADC cannot be calculated. But when there is an adequate quota of ventilated units, ADC values are obtained. Thus, while a mixed region containing both collapsed and overdistended airspaces may show no change or an increase in average x-ray attenuation, it will display the sort of abnormally high ADC observed here.

Methodological limitations

Limitations of the HP MRI methodology are relevant to understanding our results. ADC cannot discriminate between the alveoli and the alveolar ducts and cannot identify changes in alveolar shape that may contribute to the dynamics of lung inflation (111). By measuring the longitudinal and transverse components of gas diffusion, investigators using HP MRI have observed decreases in alveolar depth and dilatation of the alveolar ducts during inspiration in healthy humans (100). While a single ADC value cannot capture these phenomena entirely, this limitation should not diminish the relevance of our findings, as an elevated ADC signal during atelectasis is likely a marker of pathological maldistribution of inflation within the acinus. Furthermore, alveolar ducts are likely to be less important than alveoli in acinar diffusion (112).

Validation of ADC in the measurement of alveolar size has only been performed in healthy and emphysematous lungs (74). However, findings comparable with our observations—including airspace expansion during atelectasis and contraction during recruitment—have been described in studies using a variety of techniques, supporting our interpretation (91, 98, 113, 114).

Future Directions of HP MRI in Respiratory Failure

Overall, HP MRI studies (82-84) suggest that increased ADC is a marker of airspace overdistension caused by atelectasis. When recruitment occurs, airspace stretch is reduced, rather than worsened, by higher airway pressures. Whether this effect has consequences on pulmonary biology and outcomes is unclear. Since lung hyperinflation by high VT is a recognized trigger of VALI (29), atelectasis-related overdistension could be an important component of this injury. HP MRI research can productively contribute to the further elucidation of these dynamics in a number of ways.

A particularly appealing development of HP MRI techniques is the ability to study metabolic activity using HP ^{13}C-labeled molecules such as pyruvate. Intravenously injected ^{13}C-labeled pyruvate can be used to obtain regional maps of tissue metabolic activity(115, 116). When matched with corresponding maps of ADC, a complete description of pulmonary stretch and its metabolic and biological consequences will be available.

Furthermore, HP MRI could make a substantial contribution to the identification of injury types and patient subpopulations that favorably respond to attempts to minimize airspace distension through recruitment. Application of PEEP may attenuate the evolution of lung inflammation under the condition that it mitigates airspace stretch (rather than worsens it) by increasing the number of ventilated airspaces. However, in deciding to use PEEP to stem inflammation, one must take into account several complexities. For one, ARDS lungs are more heterogeneous than animal models; as a result, healthy lung regions at distance from atelectasis may be injured by higher pressures. Second, only a minority of patients with established ARDS have significant amounts of recruitable lung tissue. And third, high PEEP complicates fluid and hemodynamic management (117).

Another possible use for HP MRI is the clarification of the roles of VT and recruitment strategies in patients who do not have ARDS or have a milder form of this condition. It is not clear if harmful levels of lung stretch can be reached in these circumstances when moderately large tidal volumes are used. Such VT values (i.e. 10-12 ml/kg) do not cause VALI in healthy animals (118). Yet moderate VT has been shown to worsen pulmonary outcomes in patients without previous lung injury, as opposed to lower VT and moderate PEEP (119). In ventilated mice, PEEP prevented the harmful effects of very high VT ventilation (120). This protective capacity of PEEP seems to be due to the fact that atelectasis regionally amplifies the effects of tidal volume on airspace stretch; in other words, lungs can be injured by even a relatively small VT if poor recruitment is not adequately addressed (121). HP MRI could provide an essential contribution to the study of the interaction between PEEP and VT by clarifying their mutual effects on airspace dimensions. Combining all these HP MRI capabilities may in the near future provide conclusive answers to the many uncertainties about mechanical ventilation and acute respiratory failure.

Acknowledgments

We would like to acknowledge BLES Biochemicals (London, Ontario, Canada) for donating the surfactant formulation used in our experiments.

Funding: this work was supported by National Institutes of Health (Bethesda, MD, USA) grants R01-HL064741 and R01-HL077241. Dr Cereda is supported by a grant from the Foundation for Anesthesia Education and Research (Rochester, MN, USA) and the Society of Critical Care Anesthesiologists (Park Ridge, IL, USA).

References

1. Duggan M, Kavanagh BP. Pulmonary atelectasis: a pathogenic perioperative entity. Anesthesiology. 2005; 102:838–854. [PubMed: 15791115]
2. Matthay MA, Ware LB, Zimmerman GA. The acute respiratory distress syndrome. J Clin Invest. 2012; 122:2731–2740. [PubMed: 22850883]
3. Ranieri VM, Rubenfeld GD, Thompson BT, Ferguson ND, Caldwell E, Fan E, Camporota L, Slutsky AS. ARDS Definition Task Force. Acute respiratory distress syndrome: the Berlin Definition. JAMA. 2012; 307:2526–2533. [PubMed: 22797452]
4. Rubenfeld GD, Caldwell E, Peabody E, Weaver J, Martin DP, Neff M, Stern EJ, Hudson LD. Incidence and outcomes of acute lung injury. N Engl J Med. 2005; 353:1685–1693. [PubMed: 16236739]
5. Needham DM, Colantuoni E, Mendez-Tellez PA, Dinglas VD, Sevransky JD, Dennison Himmelfarb CR, Desai SV, Shanholtz C, Brower RG, Pronovost PJ. Lung protective mechanical ventilation and two year survival in patients with acute lung injury: prospective cohort study. BMJ. 2012; 344:e2124. [PubMed: 22491953]
6. Herridge MS, Tansey CM, Matte A, Tomlinson G, Diaz-Granados N, Cooper A, Guest CB, Mazer CD, Mehta S, Stewart TE, Kudlow P, Cook D, Slutsky AS, Cheung AM. Canadian Critical Care Trials Group. Functional disability 5 years after acute respiratory distress syndrome. N Engl J Med. 2011; 364:1293–1304. [PubMed: 21470008]
7. Gattinoni L, Caironi P, Cressoni M, Chiumello D, Ranieri VM, Quintel M, Russo S, Patroniti N, Cornejo R, Bugedo G. Lung recruitment in patients with the acute respiratory distress syndrome. N Engl J Med. 2006; 354:1775–1786. [PubMed: 16641394]
8. Malbouisson LM, Muller JC, Constantin JM, Lu Q, Puybasset L, Rouby JJ. CT Scan ARDS Study Group. Computed tomography assessment of positive end-expiratory pressure-induced alveolar recruitment in patients with acute respiratory distress syndrome. Am J Respir Crit Care Med. 2001; 163:1444–1450. [PubMed: 11371416]

9. Hedenstierna G, Tokics L, Strandberg A, Lundquist H, Brismar B. Correlation of gas exchange impairment to development of atelectasis during anaesthesia and muscle paralysis. Acta Anaesthesiol Scand. 1986; 30:183–191. [PubMed: 3085429]
10. de Prost N, Costa EL, Wellman T, Musch G, Winkler T, Tucci MR, Harris RS, Venegas JG, Vidal Melo MF. Effects of surfactant depletion on regional pulmonary metabolic activity during mechanical ventilation. J Appl Physiol. 2011; 111:1249–1258. [PubMed: 21799132]
11. Tucci MR, Costa EL, Wellman TJ, Musch G, Winkler T, Harris RS, Venegas JG, Amato MB, Melo MF. Regional lung derecruitment and inflammation during 16 hours of mechanical ventilation in supine healthy sheep. Anesthesiology. 2013; 119:156–165. [PubMed: 23535501]
12. Tusman G, Bohm SH, Tempra A, Melkun F, Garcia E, Mulder PG, Lachmann B. Effects of recruitment maneuver on atelectasis in anesthetized children. Anesthesiology. 2003; 98:14–22. [PubMed: 12502973]
13. Wolf GK, Gomez-Laberge C, Rettig JS, Vargas SO, Smallwood CD, Prabhu SP, Vitali SH, Zurakowski D, Arnold JH. Mechanical ventilation guided by electrical impedance tomography in experimental acute lung injury. Crit Care Med. 2013; 41:1296–1304. [PubMed: 23474677]
14. Bouhemad B, Brisson H, Le-Guen M, Arbelot C, Lu Q, Rouby JJ. Bedside ultrasound assessment of positive end-expiratory pressure-induced lung recruitment. Am J Respir Crit Care Med. 2011; 183:341–347. [PubMed: 20851923]
15. Bendixen HH, Hedley-Whyte J, Laver MB. Impaired oxygenation in surgical patients during general anesthesia with controlled ventilation. A concept of atelectasis. N Engl J Med. 1963; 269:991–996. [PubMed: 14059732]
16. Strandberg A, Tokics L, Brismar B, Lundquist H, Hedenstierna G. Atelectasis during anaesthesia and in the postoperative period. Acta Anaesthesiol Scand. 1986; 30:154–158. [PubMed: 3705902]
17. Egbert LD, Laver MB, Bendixen HH. Intermittent deep breaths and compliance during anesthesia in man. Anesthesiology. 1963; 24:57–66.
18. Hedenstierna G, Strandberg A, Brismar B, Lundquist H, Svensson L, Tokics L. Functional residual capacity, thoracoabdominal dimensions, and central blood volume during general anesthesia with muscle paralysis and mechanical ventilation. Anesthesiology. 1985; 62:247–254. [PubMed: 3977112]
19. Rothen HU, Sporre B, Engberg G, Wegenius G, Hogman M, Hedenstierna G. Influence of gas composition on recurrence of atelectasis after a reexpansion maneuver during general anesthesia. Anesthesiology. 1995; 82:832–842. [PubMed: 7717553]
20. Lundquist H, Hedenstierna G, Strandberg A, Tokics L, Brismar B. CT-assessment of dependent lung densities in man during general anaesthesia. Acta Radiol. 1995; 36:626–632. [PubMed: 8519574]
21. Guerin C, Reignier J, Richard JC, Beuret P, Gacouin A, Boulain T, Mercier E, Badet M, Mercat A, Baudin O, Clavel M, Chatellier D, Jaber S, Rosselli S, Mancebo J, Sirodot M, Hilbert G, Bengler C, Richecoeur J, Gainnier M, Bayle F, Bourdin G, Leray V, Girard R, Baboi L, Ayzac L. PROSEVA Study Group. Prone positioning in severe acute respiratory distress syndrome. N Engl J Med. 2013; 368:2159–2168. [PubMed: 23688302]
22. Richter T, Bellani G, Scott Harris R, Vidal Melo MF, Winkler T, Venegas JG, Musch G. Effect of prone position on regional shunt, aeration, and perfusion in experimental acute lung injury. Am J Respir Crit Care Med. 2005; 172:480–487. [PubMed: 15901611]
23. Foti G, Cereda M, Sparacino ME, De Marchi L, Villa F, Pesenti A. Effects of periodic lung recruitment maneuvers on gas exchange and respiratory mechanics in mechanically ventilated acute respiratory distress syndrome (ARDS) patients. Intensive Care Med. 2000; 26:501–507. [PubMed: 10923722]
24. Pelosi P, Cadringher P, Bottino N, Panigada M, Carrieri F, Riva E, Lissoni A, Gattinoni L. Sigh in acute respiratory distress syndrome. Am J Respir Crit Care Med. 1999; 159:872–880. [PubMed: 10051265]
25. Reinius H, Jonsson L, Gustafsson S, Sundbom M, Duvernoy O, Pelosi P, Hedenstierna G, Freden F. Prevention of atelectasis in morbidly obese patients during general anesthesia and paralysis: a computerized tomography study. Anesthesiology. 2009; 111:979–987. [PubMed: 19809292]

26. Tremblay L, Valenza F, Ribeiro SP, Li J, Slutsky AS. Injurious ventilatory strategies increase cytokines and c-fos m-RNA expression in an isolated rat lung model. J Clin Invest. 1997; 99:944–952. [PubMed: 9062352]
27. Muscedere JG, Mullen JB, Gan K, Slutsky AS. Tidal ventilation at low airway pressures can augment lung injury. Am J Respir Crit Care Med. 1994; 149:1327–1334. [PubMed: 8173774]
28. Frank JA, Gutierrez JA, Jones KD, Allen L, Dobbs L, Matthay MA. Low tidal volume reduces epithelial and endothelial injury in acid-injured rat lungs. Am J Respir Crit Care Med. 2002; 165:242–249. [PubMed: 11790662]
29. Tremblay LN, Slutsky AS. Ventilator-induced lung injury: from the bench to the bedside. Intensive Care Med. 2006; 32:24–33. [PubMed: 16231069]
30. Gattinoni L, Pesenti A. The concept of “baby lung”. Intensive Care Med. 2005; 31:776–784. [PubMed: 15812622]
31. Ventilation with lower tidal volumes as compared with traditional tidal volumes for acute lung injury and the acute respiratory distress syndrome. The Acute Respiratory Distress Syndrome Network. N Engl J Med. 2000; 342:1301–1308. [PubMed: 10793162]
32. Steinberg JM, Schiller HJ, Halter JM, Gatto LA, Lee HM, Pavone LA, Nieman GF. Alveolar instability causes early ventilator-induced lung injury independent of neutrophils. Am J Respir Crit Care Med. 2004; 169:57–63. [PubMed: 14695106]
33. Vieira SR, Puybasset L, Richecoeur J, Lu Q, Cluzel P, Gusman PB, Coriat P, Rouby JJ. A lung computed tomographic assessment of positive end-expiratory pressure-induced lung overdistension. Am J Respir Crit Care Med. 1998; 158:1571–1577. [PubMed: 9817710]
34. Vieira SR, Puybasset L, Lu Q, Richecoeur J, Cluzel P, Coriat P, Rouby JJ. A scanographic assessment of pulmonary morphology in acute lung injury. Significance of the lower inflection point detected on the lung pressure-volume curve. Am J Respir Crit Care Med. 1999; 159:1612–1623. [PubMed: 10228135]
35. Brower RG, Lanken PN, MacIntyre N, Matthay MA, Morris A, Ancukiewicz M, Schoenfeld D, Thompson BT. National Heart, Lung, and Blood Institute ARDS Clinical Trials Network. Higher versus lower positive end-expiratory pressures in patients with the acute respiratory distress syndrome. N Engl J Med. 2004; 351:327–336. [PubMed: 15269312]
36. Meade MO, Cook DJ, Guyatt GH, Slutsky AS, Arabi YM, Cooper DJ, Davies AR, Hand LE, Zhou Q, Thabane L, Austin P, Lapinsky S, Baxter A, Russell J, Skrobik Y, Ronco JJ, Stewart TE. Lung Open Ventilation Study Investigators. Ventilation strategy using low tidal volumes, recruitment maneuvers, and high positive end-expiratory pressure for acute lung injury and acute respiratory distress syndrome: a randomized controlled trial. JAMA. 2008; 299:637–645. [PubMed: 18270352]
37. Mercat A, Richard JC, Vielle B, Jaber S, Osman D, Diehl JL, Lefrant JY, Richecoeur J, Nieszkowska A, Gervais C, Baudot J, Bouadma L, Brochard L. Expiratory Pressure (Express) Study Group. Positive end-expiratory pressure setting in adults with acute lung injury and acute respiratory distress syndrome: a randomized controlled trial. JAMA. 2008; 299:646–655. [PubMed: 18270353]
38. Terragni PP, Rosboch G, Tealdi A, Corno E, Menaldo E, Davini O, Gandini G, Herrmann P, Mascia L, Quintel M, Slutsky AS, Gattinoni L, Ranieri VM. Tidal hyperinflation during low tidal volume ventilation in acute respiratory distress syndrome. Am J Respir Crit Care Med. 2007; 175:160–166. [PubMed: 17038660]
39. Mattingley JS, Holets SR, Oeckler RA, Stroetz RW, Buck CF, Hubmayr RD. Sizing the lung of mechanically ventilated patients. Crit Care. 2011; 15:R60. [PubMed: 21320330]
40. Talmor D, Sarge T, Malhotra A, O'Donnell CR, Ritz R, Lisbon A, Novack V, Loring SH. Mechanical ventilation guided by esophageal pressure in acute lung injury. N Engl J Med. 2008; 359:2095–2104. [PubMed: 19001507]
41. Lichtenstein D, Goldstein I, Mourgeon E, Cluzel P, Grenier P, Rouby JJ. Comparative diagnostic performances of auscultation, chest radiography, and lung ultrasonography in acute respiratory distress syndrome. Anesthesiology. 2004; 100:9–15. [PubMed: 14695718]
42. Rouby JJ, Puybasset L, Nieszkowska A, Lu Q. Acute respiratory distress syndrome: lessons from computed tomography of the whole lung. Crit Care Med. 2003; 31:S285–95. [PubMed: 12682454]

43. Gattinoni L, Caironi P, Pelosi P, Goodman LR. What has computed tomography taught us about the acute respiratory distress syndrome? Am J Respir Crit Care Med. 2001; 164:1701–1711. [PubMed: 11719313]
44. Pelosi P, Goldner M, McKibben A, Adams A, Eccher G, Caironi P, Losappio S, Gattinoni L, Marini JJ. Recruitment and derecruitment during acute respiratory failure: an experimental study. Am J Respir Crit Care Med. 2001; 164:122–130. [PubMed: 11435250]
45. Gattinoni L, Pelosi P, Vitale G, Pesenti A, D'Andrea L, Mascheroni D. Body position changes redistribute lung computed-tomographic density in patients with acute respiratory failure. Anesthesiology. 1991; 74:15–23. [PubMed: 1986640]
46. Gattinoni L, Mascheroni D, Torresin A, Marcolin R, Fumagalli R, Vesconi S, Rossi GP, Rossi F, Baglioni S, Bassi F. Morphological response to positive end expiratory pressure in acute respiratory failure. Computerized tomography study. Intensive Care Med. 1986; 12:137–142. [PubMed: 3525633]
47. Cressoni M, Cadringher P, Chiurazzi C, Amini M, Gallazzi E, Marino A, Brioni M, Carlesso E, Chiumello D, Quintel M, Bugedo G, Gattinoni L. Lung inhomogeneity in patients with acute respiratory distress syndrome. Am J Respir Crit Care Med. 2014; 189:149–158. [PubMed: 24261322]
48. Kaczka DW, Cao K, Christensen GE, Bates JH, Simon BA. Analysis of regional mechanics in canine lung injury using forced oscillations and 3D image registration. Ann Biomed Eng. 2011; 39:1112–1124. [PubMed: 21132371]
49. Robson MD, Gatehouse PD, Bydder M, Bydder GM. Magnetic resonance: an introduction to ultrashort TE (UTE) imaging. J Comput Assist Tomogr. 2003; 27:825–846. [PubMed: 14600447]
50. Bergin CJ, Glover GH, Pauly JM. Lung parenchyma: magnetic susceptibility in MR imaging. Radiology. 1991; 180:845–848. [PubMed: 1871305]
51. Shioya S, Christman R, Ailion DC, Cutillo AG, Goodrich KC. Nuclear magnetic resonance Hahn spin-echo decay (T2) in live rats with endotoxin lung injury. Magn Reson Med. 1993; 29:441–445. [PubMed: 8464359]
52. Cutillo AG, Chan PH, Ailion DC, Watanabe S, Rao NV, Hansen CB, Albertine KH, Laicher G, Durney CH. Characterization of bleomycin lung injury by nuclear magnetic resonance: correlation between NMR relaxation times and lung water and collagen content. Magn Reson Med. 2002; 47:246–256. [PubMed: 11810667]
53. Cutillo AG, Ganesan K, Ailion DC, Morris AH, Durney CH, Symko SC, Christman RA. Alveolar air-tissue interface and nuclear magnetic resonance behavior of lung. J Appl Physiol (1985). 1991; 70:2145–2154. [PubMed: 1864797]
54. Theilmann RJ, Arai TJ, Samiee A, Dubowitz DJ, Hopkins SR, Buxton RB, Prisk GK. Quantitative MRI measurement of lung density must account for the change in T(2) (*) with lung inflation. J Magn Reson Imaging. 2009; 30:527–534. [PubMed: 19630079]
55. Mariappan YK, Glaser KJ, Hubmayr RD, Manduca A, Ehman RL, McGee KP. MR elastography of human lung parenchyma: technical development, theoretical modeling and in vivo validation. J Magn Reson Imaging. 2011; 33:1351–1361. [PubMed: 21591003]
56. McGee KP, Mariappan YK, Hubmayr RD, Carter RE, Bao Z, Levin DL, Manduca A, Ehman RL. Magnetic resonance assessment of parenchymal elasticity in normal and edematous, ventilator injured lung. J Appl Physiol. 2012
57. Chiumello D, Froio S, Bouhemad B, Camporota L, Coppola S. Clinical review: Lung imaging in acute respiratory distress syndrome patients - an update. Crit Care. 2013; 17:243. [PubMed: 24238477]
58. Musch G, Venegas JG. Positron emission tomography imaging of regional pulmonary perfusion and ventilation. Proc Am Thorac Soc. 2005; 2:522–7. [PubMed: 16352758]
59. Simon BA, Kaczka DW, Bankier AA, Parraga G. What can computed tomography and magnetic resonance imaging tell us about ventilation? J Appl Physiol (1985). 2012; 113:647–657. [PubMed: 22653989]
60. Fuld MK, Easley RB, Saba OI, Chon D, Reinhardt JM, Hoffman EA, Simon BA. CT-measured regional specific volume change reflects regional ventilation in supine sheep. J Appl Physiol (1985). 2008; 104:1177–1184. [PubMed: 18258804]

61. Hoegl S, Meinel FG, Thieme SF, Johnson TR, Eickelberg O, Zwissler B, Nikolaou K. Worsening respiratory function in mechanically ventilated intensive care patients: feasibility and value of xenon-enhanced dual energy CT. Eur J Radiol. 2013; 82:557–562. [PubMed: 23238360]

62. Deninger AJ, Mansson S, Petersson JS, Pettersson G, Magnusson P, Svensson J, Fridlund B, Hansson G, Erjefeldt I, Wollmer P, Golman K. Quantitative measurement of regional lung ventilation using 3He MRI. Magn Reson Med. 2002; 48:223–232. [PubMed: 12210930]

63. Edelman RR, Hatabu H, Tadamura E, Li W, Prasad PV. Noninvasive assessment of regional ventilation in the human lung using oxygen-enhanced magnetic resonance imaging. Nat Med. 1996; 2:1236–1239. [PubMed: 8898751]

64. Sa RC, Cronin MV, Henderson AC, Holverda S, Theilmann RJ, Arai TJ, Dubowitz DJ, Hopkins SR, Buxton RB, Prisk GK. Vertical distribution of specific ventilation in normal supine humans measured by oxygen-enhanced proton MRI. J Appl Physiol (1985). 2010; 109:1950–1959. [PubMed: 20930129]

65. Bayat S, Porra L, Albu G, Suhonen H, Strengell S, Suortti P, Sovijarvi A, Petak F, Habre W. Effect of positive end-expiratory pressure on regional ventilation distribution during mechanical ventilation after surfactant depletion. Anesthesiology. 2013; 119:89–100. [PubMed: 23559029]

66. Schuster DP, Anderson C, Kozlowski J, Lange N. Regional pulmonary perfusion in patients with acute pulmonary edema. J Nucl Med. 2002; 43:863–870. [PubMed: 12097454]

67. Musch G, Bellani G, Vidal Melo MF, Harris RS, Winkler T, Schroeder T, Venegas JG. Relation between shunt, aeration, and perfusion in experimental acute lung injury. Am J Respir Crit Care Med. 2008; 177:292–300. [PubMed: 17932380]

68. Gust R, McCarthy TJ, Kozlowski J, Stephenson AH, Schuster DP. Response to inhaled nitric oxide in acute lung injury depends on distribution of pulmonary blood flow prior to its administration. Am J Respir Crit Care Med. 1999; 159:563–570. [PubMed: 9927374]

69. Musch G, Harris RS, Vidal Melo MF, O'Neill KR, Layfield JD, Winkler T, Venegas JG. Mechanism by which a sustained inflation can worsen oxygenation in acute lung injury. Anesthesiology. 2004; 100:323–330. [PubMed: 14739807]

70. Musch G, Venegas JG, Bellani G, Winkler T, Schroeder T, Petersen B, Harris RS, Melo MF. Regional gas exchange and cellular metabolic activity in ventilator-induced lung injury. Anesthesiology. 2007; 106:723–735. [PubMed: 17413910]

71. de Prost N, Costa EL, Wellman T, Tucci G, Musch MR, Winkler T, Harris RS, Venegas JG, Kavanagh BP, Vidal Melo MF. Effects of ventilation strategy on distribution of lung inflammatory cell activity. Crit Care. 2013; 17:R175. [PubMed: 23947920]

72. Bellani G, Guerra L, Musch G, Zanella A, Patroniti N, Mauri T, Messa C, Pesenti A. Lung regional metabolic activity and gas volume changes induced by tidal ventilation in patients with acute lung injury. Am J Respir Crit Care Med. 2011; 183:1193–1199. [PubMed: 21257791]

73. Fain SB, Korosec FR, Holmes JH, O'Halloran R, Sorkness RL, Grist TM. Functional lung imaging using hyperpolarized gas MRI. J Magn Reson Imaging. 2007; 25:910–923. [PubMed: 17410561]

74. Woods JC, Choong CK, Yablonskiy DA, Bentley J, Wong J, Pierce JA, Cooper JD, Macklem PT, Conradi MS, Hogg JC. Hyperpolarized 3He diffusion MRI and histology in pulmonary emphysema. Magn Reson Med. 2006; 56:1293–1300. [PubMed: 17058206]

75. Nieman GF. Amelia Earhart, alveolar mechanics, and other great mysteries. J Appl Physiol. 2012; 112:935–936. [PubMed: 22162530]

76. Butler JP, Loring SH, Patz S, Tsuda A, Yablonskiy DA, Mentzer SJ. Evidence for adult lung growth in humans. N Engl J Med. 2012; 367:244–247. [PubMed: 22808959]

77. Saam BT, Yablonskiy DA, Kodibagkar VD, Leawoods JC, Gierada DS, Cooper JD, Lefrak SS, Conradi MS. MR imaging of diffusion of (3)He gas in healthy and diseased lungs. Magn Reson Med. 2000; 44:174–179. [PubMed: 10918314]

78. Chen XJ, Moller HE, Chawla MS, Cofer GP, Driehuys B, Hedlund LW, Johnson GA. Spatially resolved measurements of hyperpolarized gas properties in the lung in vivo. Part I: diffusion coefficient. Magn Reson Med. 1999; 42:721–728. [PubMed: 10502761]

79. Salerno M, de Lange EE, Altes TA, Truwit JD, Brookeman JR, Mugler JP 3rd. Emphysema: hyperpolarized helium 3 diffusion MR imaging of the lungs compared with spirometric indexes--initial experience. Radiology. 2002; 222:252–260. [PubMed: 11756734]

80. Fain SB, Altes TA, Panth SR, Evans MD, Waters B, Mugler JP 3rd, Korosec FR, Grist TM, Silverman M, Salerno M, Owers-Bradley J. Detection of age-dependent changes in healthy adult lungs with diffusion-weighted 3He MRI. Acad Radiol. 2005; 12:1385–1393. [PubMed: 16253850]
81. Emami K, Cadman RV, Woodburn JM, Fischer MC, Kadlecek SJ, Zhu J, Pickup S, Guyer RA, Law M, Vahdat V, Friscia ME, Ishii M, Yu J, Gefter WB, Shrager JB, Rizi RR. Early changes of lung function and structure in an elastase model of emphysema--a hyperpolarized 3He MRI study. J Appl Physiol. 2008; 104:773–786. [PubMed: 18063806]
82. Cereda M, Emami K, Kadlecek S, Xin Y, Mongkolwisetwara P, Profka H, Barulic A, Pickup S, Mansson S, Wollmer P, Ishii M, Deutschman CS, Rizi RR. Quantitative imaging of alveolar recruitment with hyperpolarized gas MRI during mechanical ventilation. J Appl Physiol. 2011; 110:499–511. [PubMed: 21127207]
83. Cereda M, Xin Y, Emami K, Huang J, Rajaei J, Profka H, Han B, Mongkolwisetwara P, Kadlecek S, Kuzma NN, Pickup S, Kavanagh BP, Deutschman CS, Rizi RR. Positive End-expiratory Pressure Increments during Anesthesia in Normal Lung Result in Hysteresis and Greater Numbers of Smaller Aerated Airspaces. Anesthesiology. 2013; 119:1402–1409. [PubMed: 24025616]
84. Cereda M, Emami K, Xin Y, Kadlecek S, Kuzma NN, Mongkolwisetwara P, Profka H, Pickup S, Ishii M, Kavanagh BP, Deutschman CS, Rizi RR. Imaging the interaction of atelectasis and overdistension in surfactant-depleted lungs. Crit Care Med. 2013; 41:527–535. [PubMed: 23263577]
85. Hamedani H, Kadlececk S, Han B, Emami K, Xin Y, Ishii M, Rossman M, Rizi R. A multiple-breath³He wash-in regimen to reduce the limitation of 3He pAO₂-imaging due to delayed ventilation and slow filling. 2013:4161.
86. Carrero-Gonzalez L, Kaulisch T, Ruiz-Cabello J, Perez-Sanchez JM, Peces-Barba G, Stiller D, Rodriguez I. Apparent diffusion coefficient of hyperpolarized (3) He with minimal influence of the residual gas in small animals. NMR Biomed. 2012
87. Duggan M, McCaul CL, McNamara PJ, Engelberts D, Ackerley C, Kavanagh BP. Atelectasis causes vascular leak and lethal right ventricular failure in uninjured rat lungs. Am J Respir Crit Care Med. 2003; 167:1633–1640. [PubMed: 12663325]
88. Rudolph A, Markstaller K, Gast KK, David M, Schreiber WG, Eberle B. Visualization of alveolar recruitment in a porcine model of unilateral lung lavage using 3He-MRI. Acta Anaesthesiol Scand. 2009; 53:1310–1316. [PubMed: 19681783]
89. Thomas AC, Nouls JC, Driehuys B, Voltz JW, Fubara B, Foley J, Bradbury JA, Zeldin DC. Ventilation defects observed with hyperpolarized 3He magnetic resonance imaging in a mouse model of acute lung injury. Am J Respir Cell Mol Biol. 2011; 44:648–654. [PubMed: 20595465]
90. Mead J, Takishima T, Leith D. Stress distribution in lungs: a model of pulmonary elasticity. J Appl Physiol. 1970; 28:596–608. [PubMed: 5442255]
91. Lum H, Huang I, Mitzner W. Morphological evidence for alveolar recruitment during inflation at high transpulmonary pressure. J Appl Physiol. 1990; 68:2280–2286. [PubMed: 2384408]
92. Hickling KG. Best compliance during a decremental, but not incremental, positive end-expiratory pressure trial is related to open-lung positive end-expiratory pressure: a mathematical model of acute respiratory distress syndrome lungs. Am J Respir Crit Care Med. 2001; 163:69–78. [PubMed: 11208628]
93. Escolar JD, Escolar A. Lung hysteresis: a morphological view. Histol Histopathol. 2004; 19:159–166. [PubMed: 14702184]
94. Storey WF, Staub NC. Ventilation of terminal air units. J Appl Physiol. 1962; 17:391–397. [PubMed: 13917520]
95. Mercer RR, Laco JM, Crapo JD. Three-dimensional reconstruction of alveoli in the rat lung for pressure-volume relationships. J Appl Physiol. 1987; 62:1480–1487. [PubMed: 3597219]
96. Bachofen H, Hildebrandt J, Bachofen M. Pressure-volume curves of air- and liquid-filled excised lungs-surface tension in situ. J Appl Physiol. 1970; 29:422–431. [PubMed: 4990020]
97. Escolar JD, Escolar MA, Guzman J, Roques M. Pressure volume curve and alveolar recruitment/de-recruitment. A morphometric model of the respiratory cycle. Histol Histopathol. 2002; 17:383–392. [PubMed: 11962742]

98. Smaldone GC, Mitzner W, Itoh H. Role of alveolar recruitment in lung inflation: influence on pressure-volume hysteresis. J Appl Physiol. 1983; 55:1321–1332. [PubMed: 6629967]

99. Carney DE, Bredenberg CE, Schiller HJ, Picone AL, McCann UG, Gatto LA, Bailey G, Fillinger M, Nieman GF. The Mechanism of Lung Volume Change during Mechanical Ventilation. Am J Respir Crit Care Med. 1999; 160:1697–1702.

100. Hajari AJ, Yablonskiy DA, Sukstanskii AL, Quirk JD, Conradi MS, Woods JC. Morphometric changes in the human pulmonary acinus during inflation. J Appl Physiol. 2012; 112:937–943. [PubMed: 22096115]

101. Carvalho AR, Jandre FC, Pino AV, Bozza FA, Salluh JI, Rodrigues R, Soares JH, Giannella-Neto A. Effects of descending positive end-expiratory pressure on lung mechanics and aeration in healthy anaesthetized piglets. Crit Care. 2006; 10:R122. [PubMed: 16925814]

102. Severgnini P, Selmo G, Lanza C, Chiesa A, Frigerio A, Bacuzzi A, Dionigi G, Novario R, Gregoretti C, de Abreu MG, Schultz MJ, Jaber S, Futier E, Chiaranda M, Pelosi P. Protective Mechanical Ventilation during General Anesthesia for Open Abdominal Surgery Improves Postoperative Pulmonary Function. Anesthesiology. 2013

103. Jaber S, Coisel Y, Chanques G, Futier E, Constantin JM, Michelet P, Beaussier M, Lefrant JY, Allaouchiche B, Capdevila X, Marret E. A multicentre observational study of intra-operative ventilatory management during general anaesthesia: tidal volumes and relation to body weight. Anaesthesia. 2012; 67:999–1008. [PubMed: 22708696]

104. Denison DM, Morgan MD, Millar AB. Estimation of regional gas and tissue volumes of the lung in supine man using computed tomography. Thorax. 1986; 41:620–628. [PubMed: 3787544]

105. Gil J, Weibel ER. Morphological study of pressure-volume hysteresis in rat lungs fixed by vascular perfusion. Respir Physiol. 1972; 15:190–213. [PubMed: 5042167]

106. Sinclair SE, Chi E, Lin HI, Altemeier WA. Positive end-expiratory pressure alters the severity and spatial heterogeneity of ventilator-induced lung injury: an argument for cyclical airway collapse. J Crit Care. 2009; 24:206–211. [PubMed: 19327294]

107. de Prost N, Costa EL, Wellman T, Musch G, Tucci MR, Winkler T, Harris RS, Venegas JG, Kavanagh BP, Vidal Melo MF. Effects of ventilation strategy on distribution of lung inflammatory cell activity. Crit Care. 2013; 17:R175. [PubMed: 23947920]

108. Lachmann B, Robertson B, Vogel J. In vivo lung lavage as an experimental model of the respiratory distress syndrome. Acta Anaesthesiol Scand. 1980; 24:231–236. [PubMed: 7445941]

109. Froese AB, McCulloch PR, Sugiura M, Vaclavik S, Possmayer F, Moller F. Optimizing alveolar expansion prolongs the effectiveness of exogenous surfactant therapy in the adult rabbit. Am Rev Respir Dis. 1993; 148:569–577. [PubMed: 8368625]

110. Krause M, Olsson T, Law AB, Parker RA, Lindstrom DP, Sundell HW, Cotton RB. Effect of volume recruitment on response to surfactant treatment in rabbits with lung injury. Am J Respir Crit Care Med. 1997; 156:862–866. [PubMed: 9310005]

111. Smaldone GC, Mitzner W. Viewpoint: unresolved mysteries. J Appl Physiol. 2012; 113:1945–1947. [PubMed: 22797308]

112. Mercer RR, Crapo JD. Three-dimensional reconstruction of the rat acinus. J Appl Physiol. 1987; 63:785–794. [PubMed: 3654440]

113. Bachofen H, Gehr P, Weibel ER. Alterations of mechanical properties and morphology in excised rabbit lungs rinsed with a detergent. J Appl Physiol. 1979; 47:1002–1010. [PubMed: 511700]

114. Namati E, Thiesse J, de Ryk J, McLennan G. Alveolar dynamics during respiration: are the pores of Kohn a pathway to recruitment? Am J Respir Cell Mol Biol. 2008; 38:572–578. [PubMed: 18096874]

115. Wiesinger F, Weidl E, Menzel MI, Janich MA, Khegai O, Glaser SJ, Haase A, Schwaiger M, Schulte RF. IDEAL spiral CSI for dynamic metabolic MR imaging of hyperpolarized [1-13C]pyruvate. Magn Reson Med. 2012; 68:8–16. [PubMed: 22127962]

116. Thind K, Chen A, Friesen-Waldner L, Ouriadov A, Scholl TJ, Fox M, Wong E, Vandyk J, Hope A, Santyr G. Detection of radiation-induced lung injury using hyperpolarized (13) C magnetic resonance spectroscopy and imaging. Magn Reson Med. 2012

117. Vieillard-Baron A, Jardin F. Why protect the right ventricle in patients with acute respiratory distress syndrome? Curr Opin Crit Care. 2003; 9:15–21. [PubMed: 12548024]

118. Wilson MR, Patel BV, Takata M. Ventilation with “clinically relevant” high tidal volumes does not promote stretch-induced injury in the lungs of healthy mice. Crit Care Med. 2012; 40:2850–2857. [PubMed: 22890257]

119. Serpa Neto A, Cardoso SO, Manetta JA, Pereira VG, Esposito DC, Pasqualucci Mde O, Damasceno MC, Schultz MJ. Association between use of lung-protective ventilation with lower tidal volumes and clinical outcomes among patients without acute respiratory distress syndrome: a meta-analysis. JAMA. 2012; 308:1651–1659. [PubMed: 23093163]

120. Seah AS, Grant KA, Aliyeva M, Allen GB, Bates JH. Quantifying the roles of tidal volume and PEEP in the pathogenesis of ventilator-induced lung injury. Ann Biomed Eng. 2011; 39:1505–1516. [PubMed: 21203845]

121. Albaiceta GM, Blanch L. Gone with the wind: the role of air flow in mucus clearance during mechanical ventilation*. Crit Care Med. 2012; 40:1013–1014. [PubMed: 22343862]

List of abbreviations

ARDS	acute respiratory distress syndrome
CT	computed tomography
PET	positron emission tomography
HP	hyperpolarized
MRI	magnetic resonance imaging
VT	tidal volume
PEEP	positive end expiratory pressure
VALI	ventilator-associated lung injury
UTE	ultra short echo time
18-FDG	[18F]-fluoro-2-deoxy-D-glucose
ADC	apparent diffusion coefficient
RF	radiofrequency

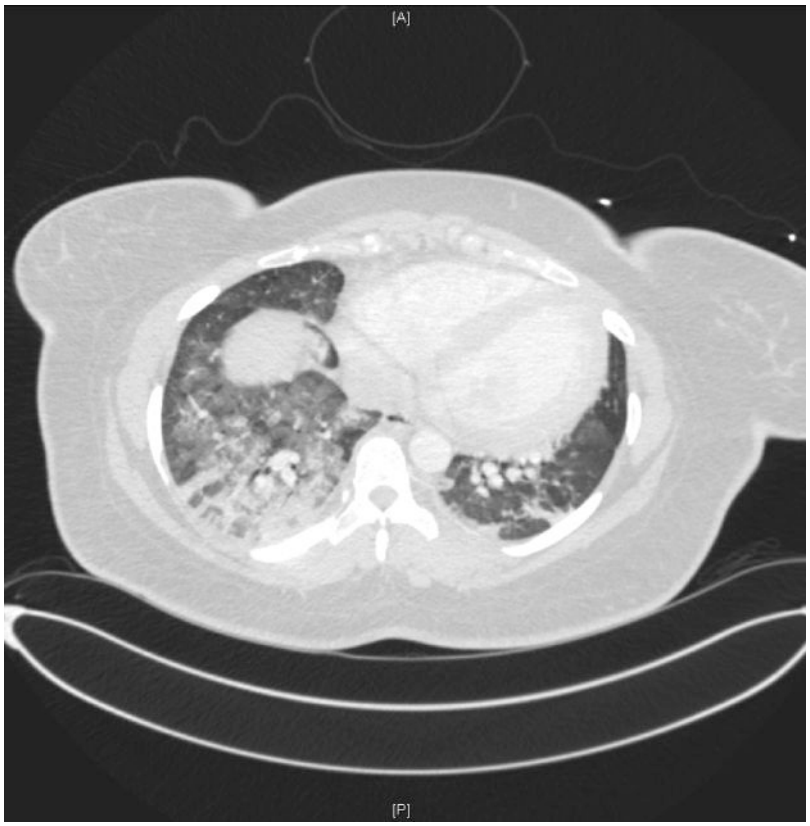

Figure 1.
Axial CT scan from a patient with acute respiratory distress syndrome (ARDS) caused by trauma and aspiration pneumonia. Prominent dorsal opacities are visible with progressive ventral to dorsal increase in CT density. Frontal lung regions are better aerated.

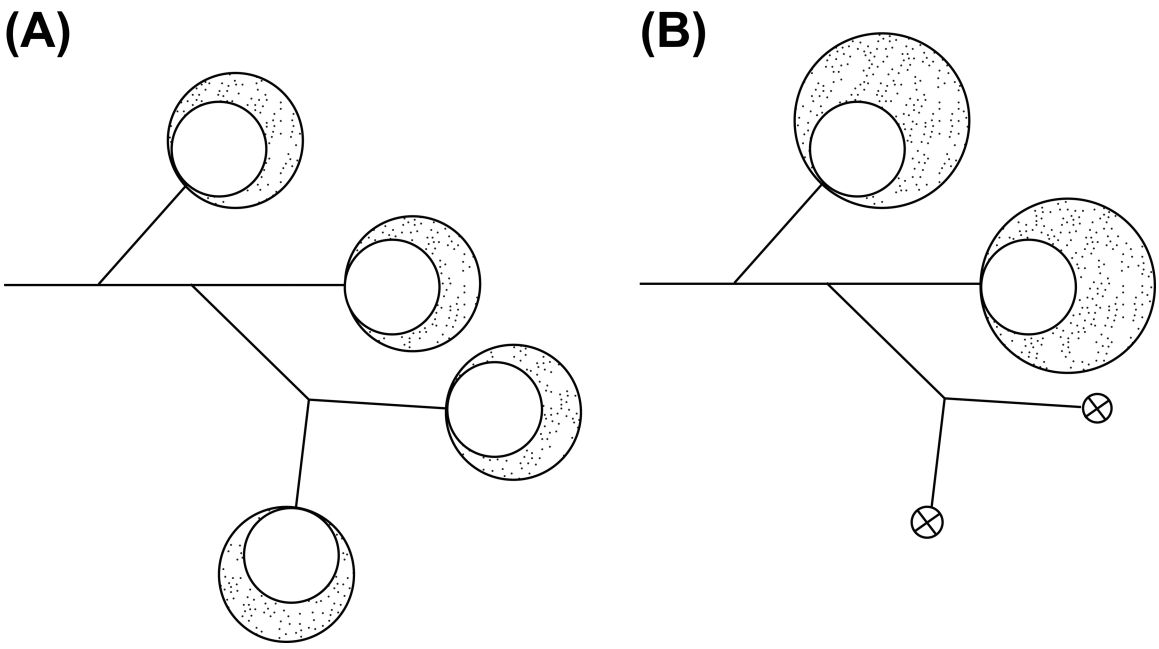

Figure 2.
Simplified model of lung aeration in normal conditions (left) and after atelectasis and lung injury (right). Alveolar collapse causes dilatation of residual ventilated airspaces.

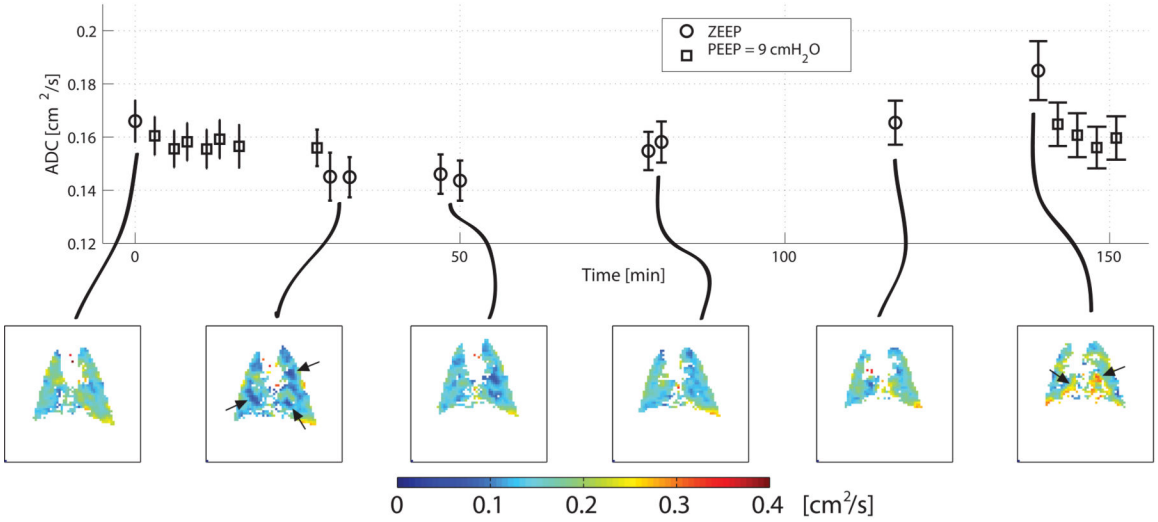

Figure 3.

Time course of apparent diffusion coefficient (ADC) for hyperpolarized ^{3}He in a rat ventilated with constant tidal volume and zero positive end-expiratory pressure for an extended time. The first and the second image were obtained before and after a recruitment maneuver, causing ADC to decrease. ADC progressively increased during subsequent ventilation, which was paralleled by increasing airway pressures (not shown). Focal changes in ADC are indicated by arrows. (Reproduced from Ref 95).

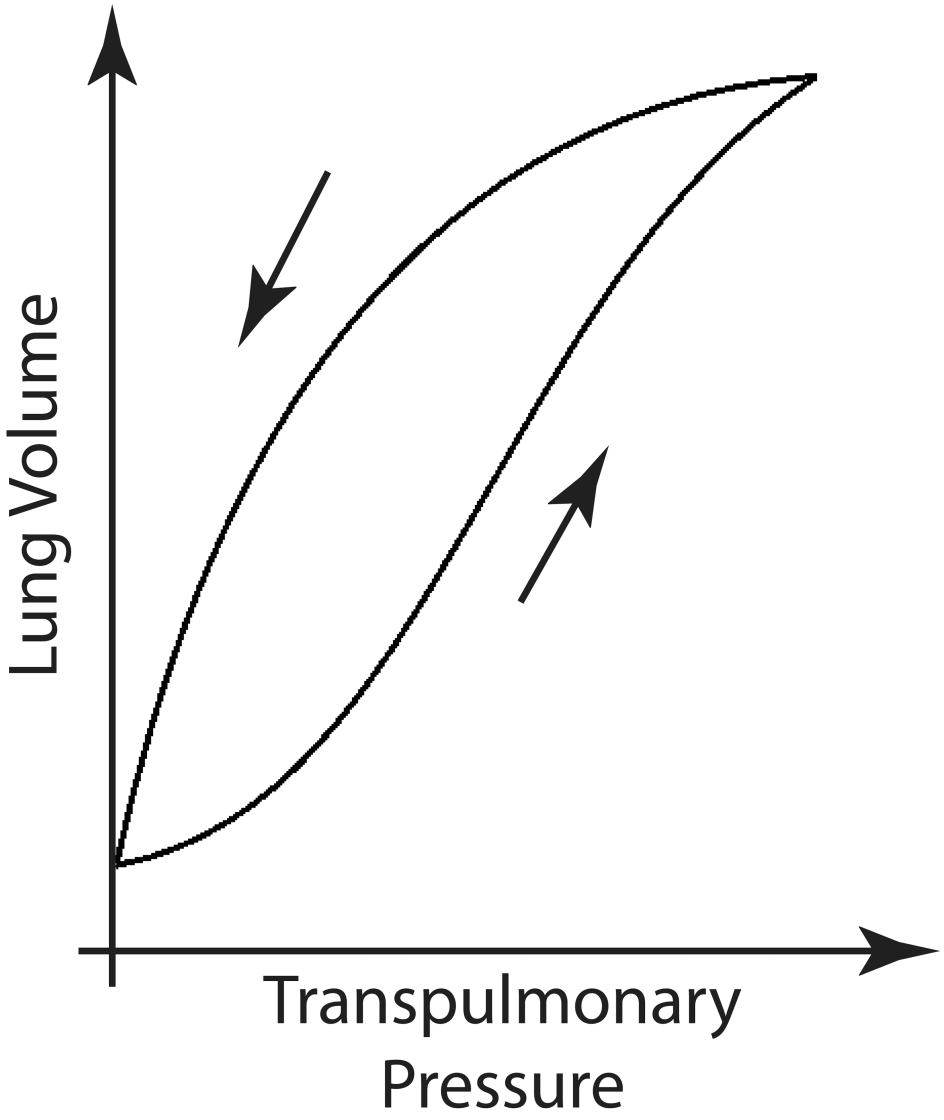

Figure 4.

Pressure volume relationship for a whole lung during an inflation-deflation cycle. The presence of pulmonary hysteresis is shown by higher lung volumes for equivalent transpulmonary pressures in the deflation vs. the deflation limb.

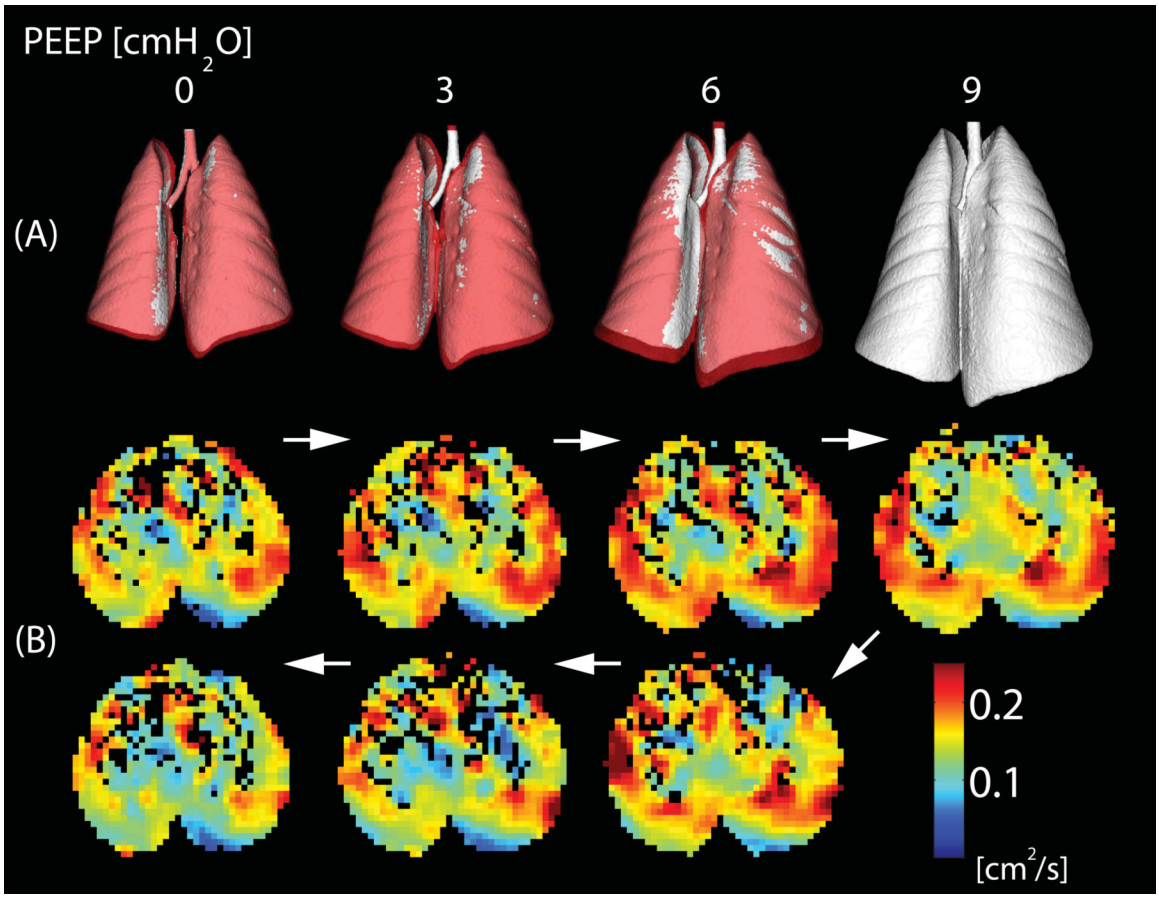

Figure 5.

A) Three-dimensional CT reconstructions of the whole lungs obtained in healthy rats while positive end expiratory pressure (PEEP) was raised from 0 to 9 cmH_2O and then lowered back to 0 cmH_2O (in steps of 3 cmH_2O). Images of the lungs during descending PEEP are shown in purple and are superimposed on the images obtained during rising PEEP (in white): the larger lung volumes during descending PEEP document hysteresis. B) Axial maps of apparent diffusion coefficient (ADC) obtained during a PEEP cycle identical to A): ADC values are lower during descending PEEP suggesting a “reverse hysteresis” of the individual airspaces. (Reproduced from Ref 96).

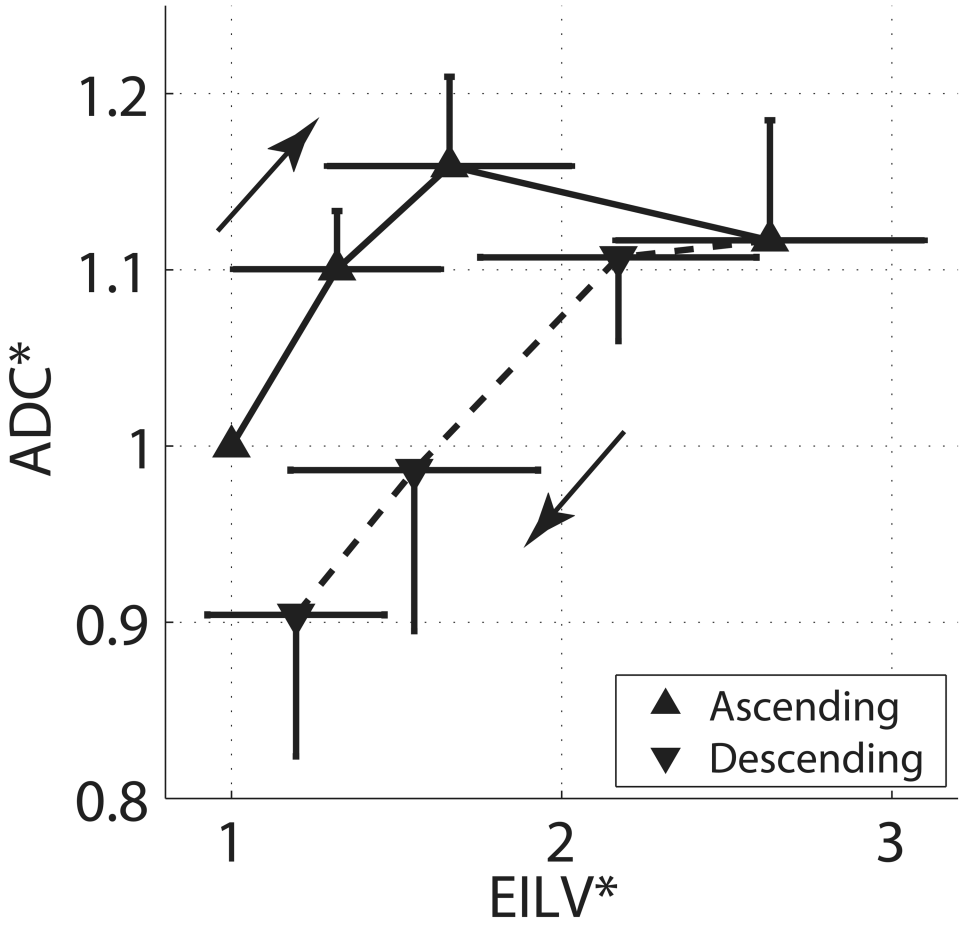

Figure 6.

Values of apparent diffusion coefficient (ADC) and end inspiratory lung volumes (EILV) during ascending and descending PEEP ramps performed as described in Figure 5. All values are expressed as fraction of baseline at positive end expiratory pressure (PEEP) of zero. Dissociation between the hysteretic behavior of the whole lung and the responses of airspace dimensions is again shown. (Reproduced from Ref 96).

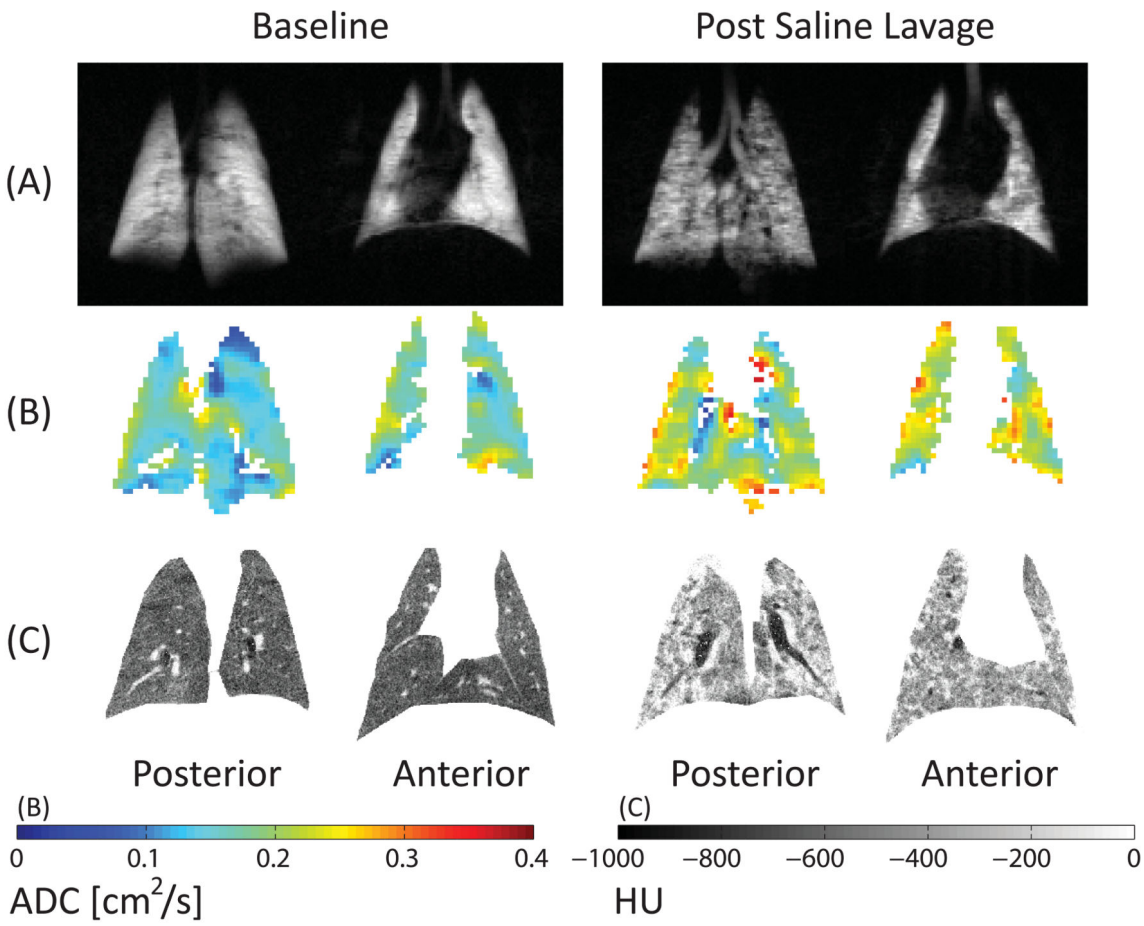

Figure 7.

Maps of ^{3}He density (top), apparent diffusion coefficient (ADC, middle) and CT density (bottom) before and after saline lavage. Color scales for diffusion (cm^2/s) and CT density (HU) are shown at the bottom. Atelectasis is documented by high CT density and low ^{3}He signal. However, ADC was increased overall and in regions of abnormally high CT density.

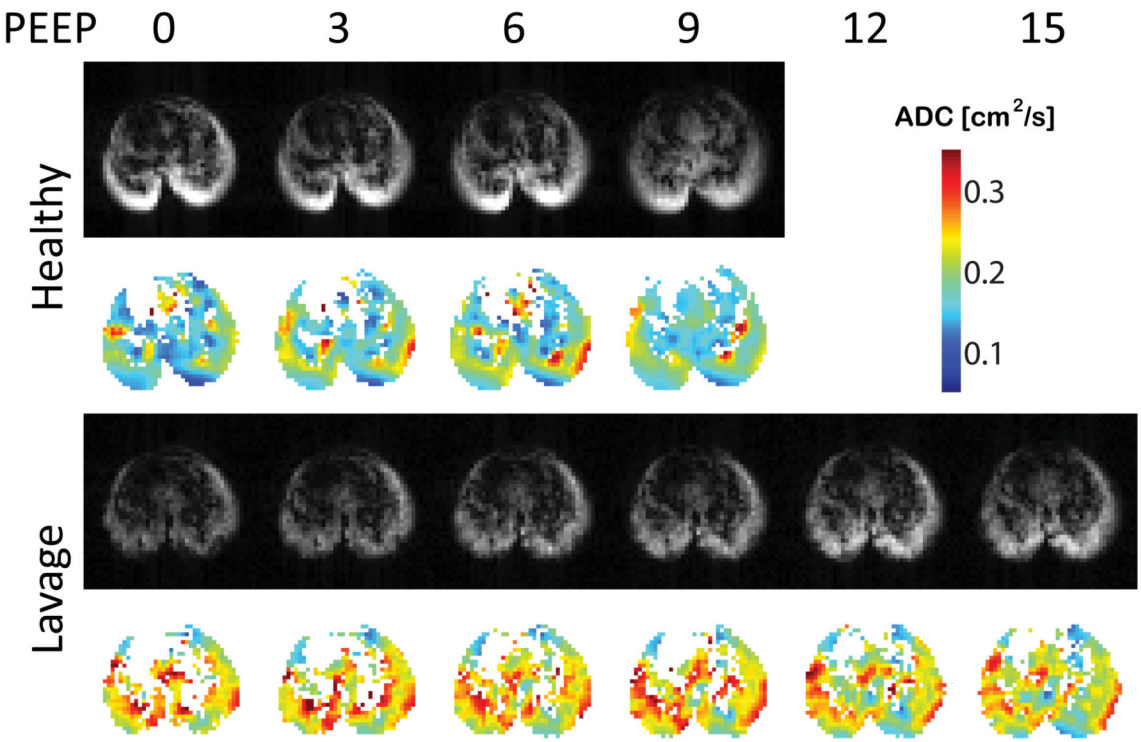

Figure 8.

ADC maps for rats ventilated at different levels of PEEP at healthy baseline (top) and after saline lavage (bottom). PEEP after saline lavage decreased ADC towards normal values (unpublished observations).